

Sub-Inertial Oscillations in the Black Sea Generated by the Semidiurnal Tidal Potential

A. N. Lukyanova^{a, *}, A. V. Bagaev^a, V. A. Ivanov^a, and V. B. Zalesny^b

^a Marine Hydrophysical Institute, Russian Academy of Sciences, Sevastopol, 299011 Russia

^b Institute of Numerical Mathematics, Russian Academy of Sciences, Moscow, 119333 Russia

*e-mail: annieromanenko@gmail.com

Received December 20, 2016; in final form, March 15, 2017

Abstract—The Black Sea shelf is a region of intense manifestation of various dynamical processes. Under the influence of different natural forces, eddy-wave phenomena develop here, which influence the general circulation of sea waters, biological productivity, and the condition of the engineering structures. Modern numerical models allow us to simulate and analyze the processes of the joint dynamics of marine circulation and large-scale waves. In this work, we study the spatiotemporal spectral characteristics of the sea level and velocity fluctuations formed due to atmospheric forcing and tidal potential. The hydrophysical fields are calculated using the Institute of Numerical Mathematics, Russian Academy of Sciences (INM RAS), σ model based on primitive equations. We use the CORE data as atmospheric forcing at the sea surface; the tidal potential is described by the semidiurnal lunar constituent M_2 . Analyzing the simulation results makes it possible to emphasize that accounting for the semidiurnal tidal potential not only improves the accuracy of the sea-level calculation at coastal stations, but also generates subinertial baroclinic oscillations previously found in the Black Sea from the data of in situ observations.

Keywords: subinertial oscillations, Black Sea, mathematical modeling

DOI: 10.1134/S000143381706007X

1. INTRODUCTION

Experimental observations in the oceanic and sea basins require large investments and return very important information in relatively low amounts. An analysis of the observations in the Black Sea allows us to distinguish the main features of the natural phenomena, reveal their individual quantitative characteristics, and describe the interesting observed peculiarities [1–3]. The methods of mathematical modeling [4–12] and joint analysis of the field data and numerical simulations [13, 14] are used in modern research for increasing the amount of information and improving the analysis of the physical processes. Numerical modeling allows us to obtain long-term time series of various characteristics with high spatial and time resolution. Knowledge of the medium-scale eddy-wave dynamics of the modeled basin [1, 2, 4] allows us to determine the degree of reliability of the results obtained in the numerical experiments and reveal the directions of model development.

The objective of this research is to investigate the internal oscillations appearing in a closed stratified marine basin under the forcing of the semidiurnal tidal potential. One specific feature of this research is the fact that these fluctuations in the Black Sea are modeled together with the processes of large-scale circulation.

The objectives of research include a calculation of spectral characteristics of fluctuations at different geographically remote regions of the Black Sea shelf with various bottom profiles. A comparison of the results with the known parameters of the baroclinic fluctuations (based on the field data and calculations using other models) allows us to classify these fluctuations. We distinguish the main effects of the influence of the semidiurnal tidal potential and confirm the hypothesis about the generation of the forced baroclinic tide and baroclinic seiches at periods smaller than the local inertial period.

2. MATHEMATICAL MODEL AND NUMERICAL SIMULATIONS

2.1. Mathematical Model

We selected the mathematical hydrodynamic model of the Black and Azov seas developed at the Institute of Numerical Mathematics of the Russian Academy of Sciences (INM RAS). The INM RAS model is based on the system of primitive equations written in the spherical coordinate system with account for the hydrostatic and Boussinesq approxi-

mations. Dimensionless variable $\sigma \in [0, 1]$ is used as the vertical coordinate:

$$\sigma = \frac{z - \zeta}{H - \zeta},$$

where ζ is the deviation of sea surface height from its unperturbed state, H is the sea depth at rest, and z is the downward physical vertical coordinate with the initial point at the unperturbed sea surface [4, 5]. The model equations are written in symmetrized form and are presented in [4].

The numerical algorithm of the model is based on the method of multicomponent splitting [6]. The method includes splitting of the model equations with respect to the physical processes and geometrical coordinates. The application of this splitting significantly increases the efficiency of calculations [4–6].

2.2. Input Data

The domain of calculations approximating the basins of the Black and Azov seas is located from $27^{\circ}26'60''$ E to $41^{\circ}45'00''$ E and from $40^{\circ}54'36''$ N to $47^{\circ}16'12''$ N. The spatial resolution of the model is $(0^{\circ}3') \times (0^{\circ}2'24'')$ by longitude and latitude, respectively, which is equal to ~ 4 km by the horizontal coordinates. Forty σ levels nonuniformly distributed by depth are specified by the vertical. The time step of calculations is 5 min. The bottom topography, initial, and boundary conditions are given in [12].

CORE data [15] are used in the model to calculate the seasonal evolution of the atmospheric forcing in the INM RAS model. The spatial resolution of the CORE data is 1.825° by longitude (192 points); the distribution by latitude is nonuniform (94 points). The results of the model validation with the climatic forcing used in the model are given in [16]. The model adequately represents the seasonal evolution of hydro-physical fields in the Black Sea and their main large-scale spatiotemporal characteristics.

2.3. Numerical simulations

The numerical experiment was performed for 1 year and 4 months. The first climatic year was used to spin up the model; the last month of the simulation was used for the analysis with a 45-min time step of the data output. The data on the kinetic energy and sea surface height were saved and analyzed.

Three datasets from regions with different bottom profiles were selected for the analysis (Fig. 1). Each of them included three sections from the shelf zone to the deepwater region (Fig. 2). A total of 17 levels (1, 2, 3, 5, 10, 15, 20, 30, 40, 50, 60, 75, 100, 150, 200, 250, and 300 m) were used over each of the sections. The sections were selected remotely located so that, judging from the values of coherence, one could make conclusions about the localizations of fluctuations.

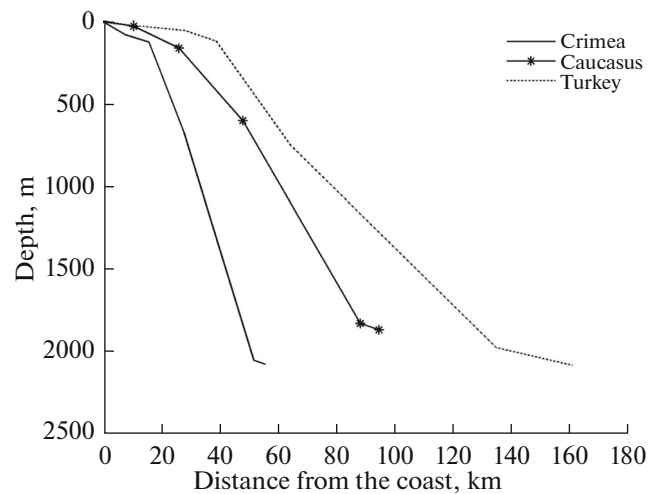


Fig. 1. Depth profiles in the three study regions.

We have calculated the Fourier spectra of sea surface height and kinetic energy fluctuations at each level using the Hamming window with 50% overlapping and calculated the Hovmöller diagrams for the velocity and sea surface height at each station. We calculated and visualized the coherence matrices between the fluctuations at the periods with maximum energy (6, 8, 12, and 17 h).

3. ANALYSIS OF CALCULATIONS

3.1. Spectral Analysis of the Sea Surface Height and Kinetic Energy

A peak at 12 h is clearly distinguished in all spectra of sea surface height fluctuations (the maximum values of the spectral amplitudes are observed in the regions of Caucasus and Turkey). This corresponds to the phase amplitude chart of the tidal oscillations, according to which an amphidromic point is located near Crimea [17, 18]. Thus, we note that the fluctuations of the sea surface height at the period of the semidiurnal tide in all spectra are maximal among all mesoscale fluctuations of the sea surface height, including the spectral amplitude of the inertial oscillations (examples in Fig. 3).

The peak of the kinetic energy at 12 h on all spectra is less pronounced when compared with the other mesoscale fluctuations. The 12-h peak of the spectra in deep-water points (2 and 3) is better manifested at points deeper than 20–30 m (Fig. 4). This provides evidence that (a) forced baroclinic fluctuations propagate at the same 12-h period as the tides; (b) these fluctuations make a significant contribution to the energy of the water motion in the low-energy layers below the main thermocline.

The spectra, which have a local maximum at a period of 12 h, were calculated from the data of climatic calculation without account for tidal forcing (sea sur-

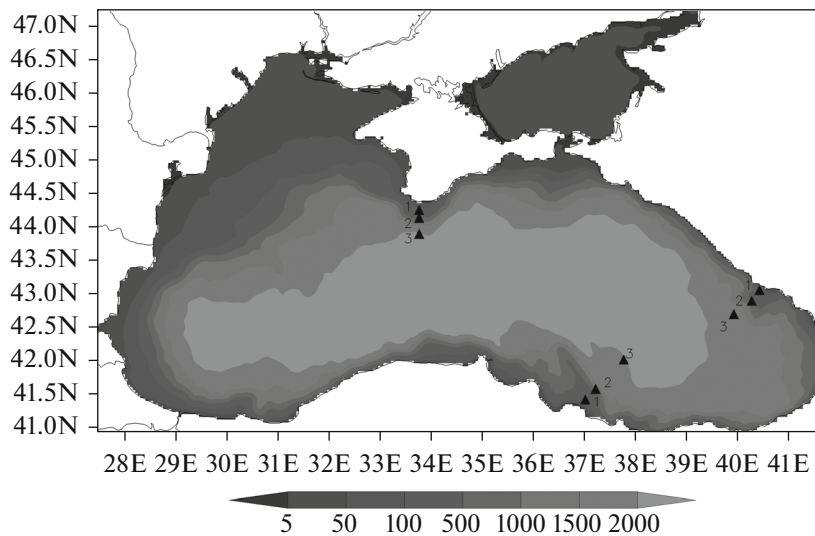


Fig. 2. Bottom topography of the Black Sea (m) and points of observations (black triangles).

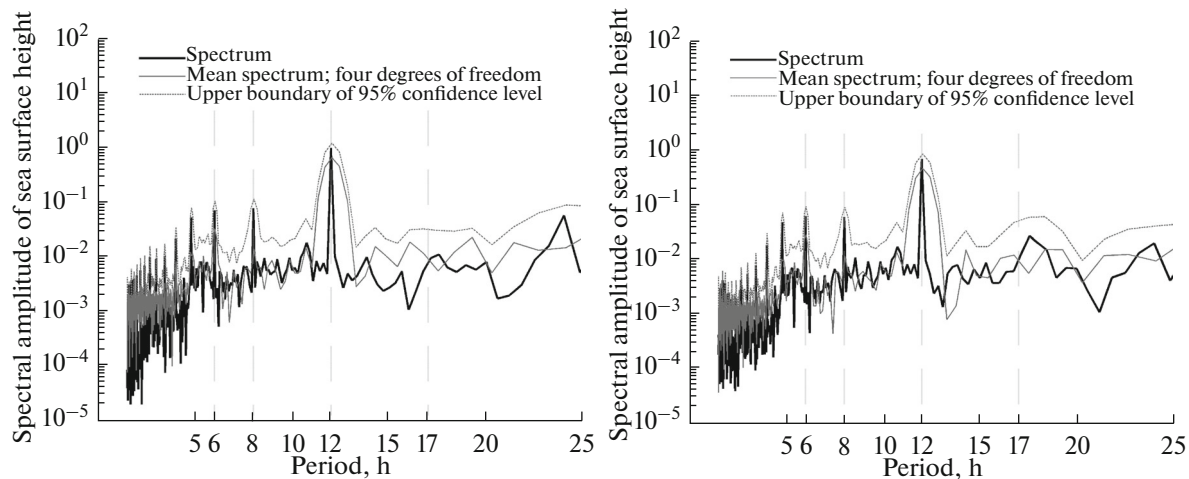


Fig. 3. Spectra of sea-level fluctuations based on the results of the numerical modeling on the second year of calculations in April in the regions of Caucasus (point 3, left panel) and Turkey (point 2, right panel).

face height at coastal points). However, its spectral amplitude is 1–2 orders of magnitude smaller than in the calculations of the sea surface height with account for the tide (Fig. 5). It is possible that this peak is related to the periodical assimilation of the atmospheric forcing. Thus, including the tidal potential increases the energy input to the total circulation of the basin, amplifying the fluctuations that are reproduced by the model at a period of 12 h.

Two stable peaks were found at periods lower than 12 h: at 6 and close to 8 h. According to [1], these periods correspond to the local baroclinic seiche fluctuations appearing in the eastern part of the sea. The characteristics of such fluctuations are determined by the peculiarities of the bottom topography and form of the coast. At deeper depths, the local maxima on the spectra are well pronounced, which may pro-

vide evidence about the baroclinic nature of these fluctuations.

3.2. Inertial Frequencies: Values of Periods

A small shift in the location of the peak near the period of the inertial motions has been observed on all plotted spectra of the kinetic energy. In the Caucasus region, where the expected natural period is 17.6 h (Table 1), approximately the same values are observed only on the shelf (~17.9 h).

At the other points, the period is stably higher (18–19 h). This fact can be explained by the influence of the permanent strong current (the Black Sea Rim Current (BSRC)). The authors of [19, 20] relate the variation in the location of the peak to the variation in the vorticity of the background current. The maxi-

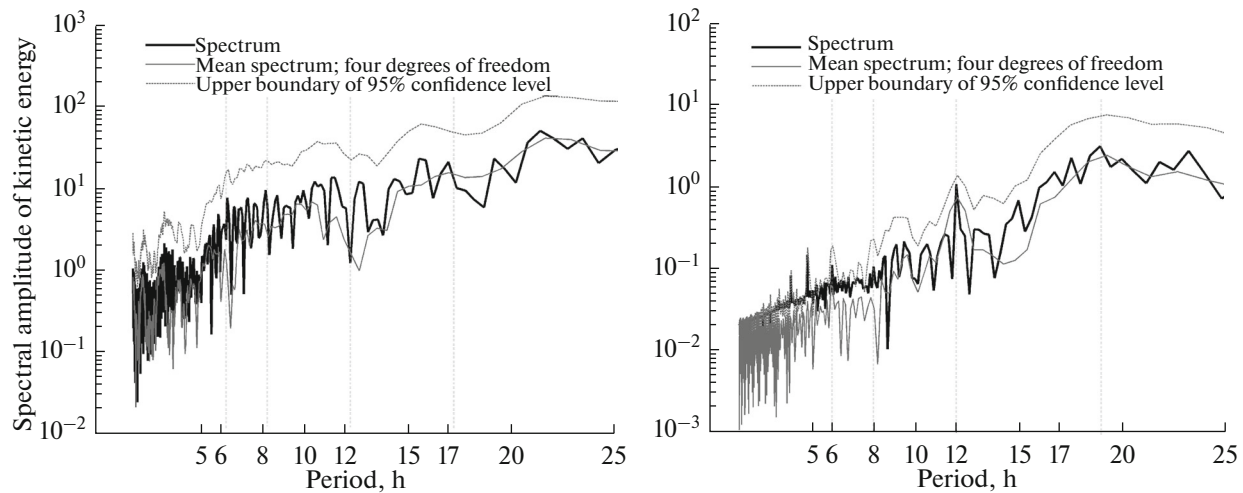


Fig. 4. Spectra of kinetic energies based on the results of the numerical modeling on the second year of calculations in April near Crimea, point 2: left panel, depth 2 m; right panel, depth 50 m.

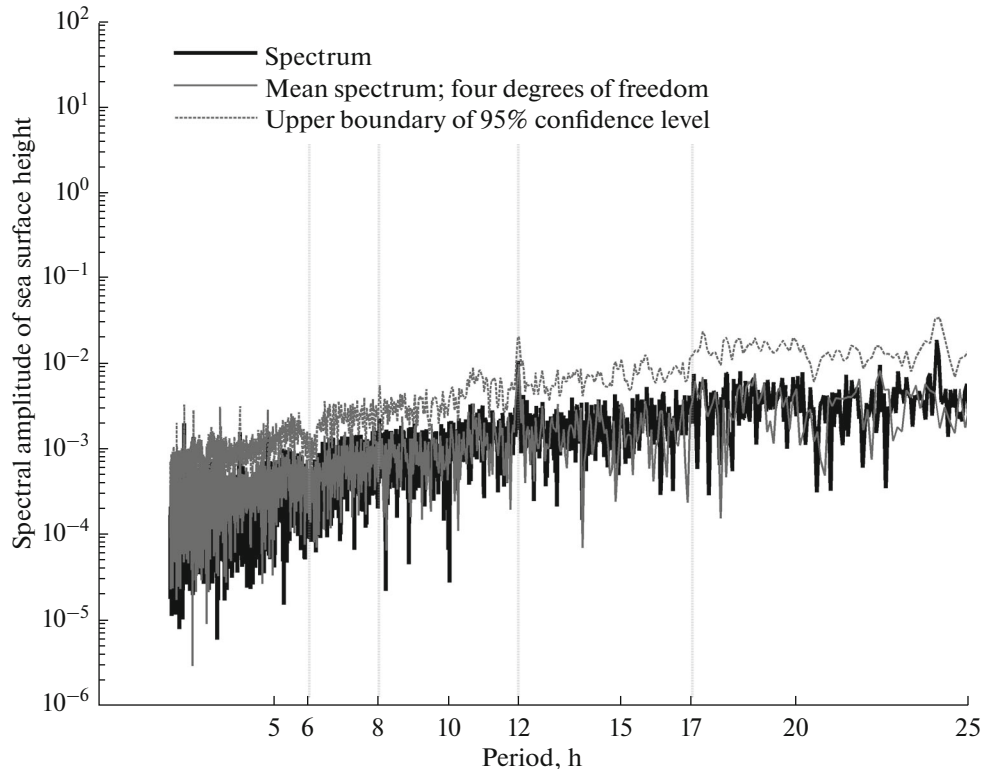


Fig. 5. Spectrum of sea level fluctuations near Yalta (numerical simulation without account for the tidal potential).

imum vorticity of the BSRC in the model is observed exactly along the Caucasus coast; it is likely that this fact causes the “red” shift in the peak, approximately by 0.08 of the inertial period.

It is interesting to note that at the deep station near the bottom the peak displaces to the “blue” range; i.e., the period of oscillations is significantly smaller than 15–17 h. This is related to the influence

of the bottom topography (trapping of waves) and, possibly, to a change in the vorticity sign [21]. At the stations near Turkey, no significant shift of the peak is observed. In the deepwater stations near Crimea, the period increases to 19 h.

Finally, we have to note that our methods of analysis may not explicitly distinguish all near-inertial oscillations (degenerated inertial-gravity and trapped

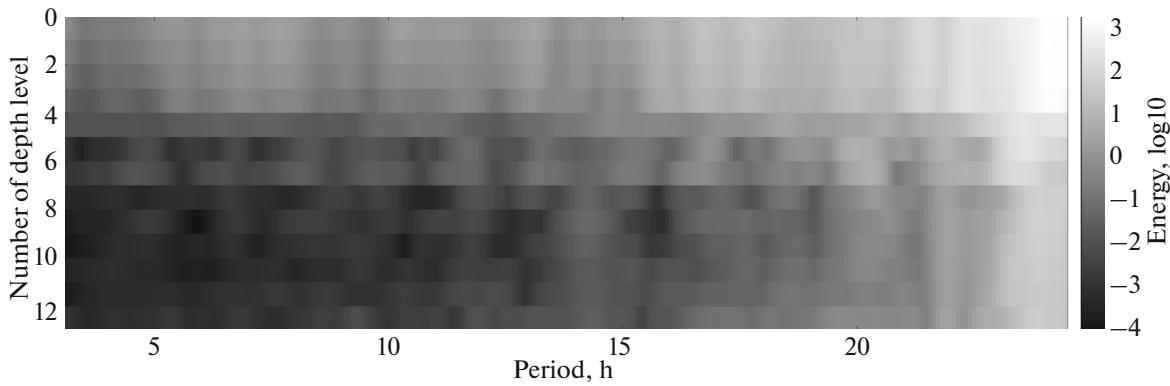


Fig. 6. Spectrogram based on the kinetic energies on the shelf of the Crimea Peninsula based on the results of numerical modeling on the second year of calculations in April. Numbers of levels are laid off along the vertical axis.

waves) which appear at periods close to 17 h and introduce distortions on the spectra [1]. In order to distinguish such fluctuations, one has to use a more frequent grid of stations and perform a wavelet analysis of the time series of observations.

3.3 Analysis of Spectrograms

According to the results of numerical modeling, the maximal energy at all levels belongs to fluctuations with a period close to 24 h (Fig. 6).

This corresponds to the previous results [1, 7] that fluctuations with a period of 24 h transport a significant part of energy in the mesoscale spectral range. As is shown in [1], the maximum energies are observed in the 0- to 5-m layer.

3.4. Analysis of Hovmöller Diagrams

The Hovmöller diagrams at all stations reveal the kinetic energy oscillations with a period of about 17 h (an example is shown in Fig. 7). These oscillations have two maxima: one is located in the surface layer (0–5 m), which is a joint response to the barotropic motions of the sea surface and influence of the tidal potential, while the second occupies deeper layers (7 m and deeper).

The propagation of oscillations occurs with a small time shift. On the one hand, this pattern of oscillations

indicates insufficient mixing in the model because the location of the pycnocline in the simulation is set too high (Fig. 8), and, on the other hand, it demonstrates the ability of the model to transfer energy of internal waves to deep layers.

A number of diagrams make it possible to trace the propagation of oscillations in the direction from the bottom to the surface, which can indicate the existence of degenerated inertial-gravity waves. It is possible that the intensification of the currents over the pycnocline occurs as a result of their breaking; however, these peculiarities require additional research.

3.5 Analysis of the Coherence between Oscillations

A very high coherence (>0.95) between sea surface height oscillations at a period of 12 h is observed at all stations. Coherence between the fluctuations of velocities in different regions and between the fluctuations of velocities and sea surface heights is lower (0.64, but rarely values of 0.8 appear). The fluctuations of velocities are also correlated in the deeper layers (beginning from the seventh level) between themselves; they are also correlated with the fluctuations of sea surface height (0.88–0.96). At a period of 17 h the coherences between the fluctuations of all measured sea surface heights and velocities are generally 0.64–0.76, which corresponds to relatively low values. It is likely related to the fact that inertial fluctuations in differing subregions of the basin have periods different from 17 h or

Table 1. Periods of inertial oscillations in the study regions

Caucasus	17.58–17.6 h	<18 h	18–18.5 h	Decreases with depth from 19 to 17 h	17 h
Turkey	17.93–18.1 h	Increases with depth from 17.5 to 18.5 h	18.5 h	17.5 h	~17 h
Crimea	17.19–17.23 h	Decreases with depth from 18.5 to 17 h	Increases with depth from 17 to 19 h	17.5 h	17 h

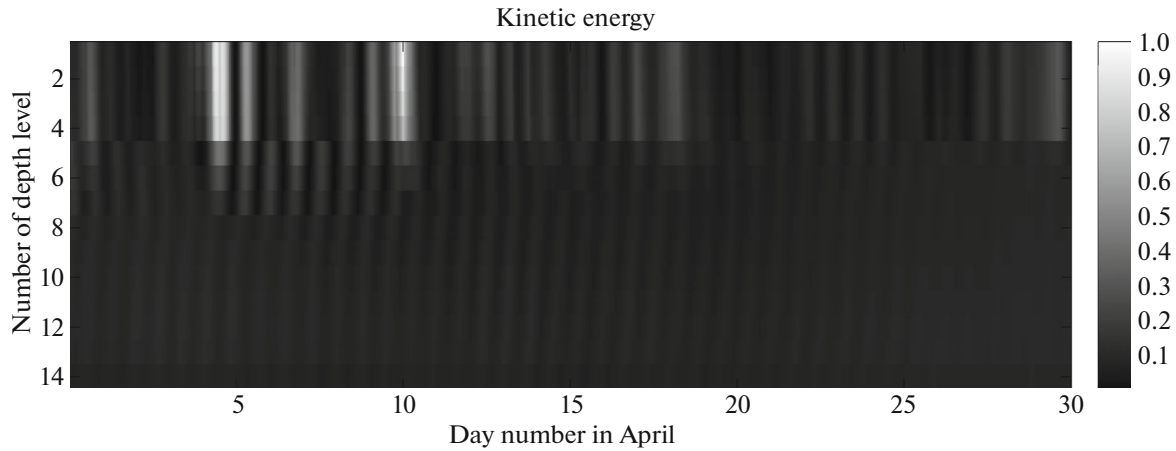


Fig. 7. Hovmöller diagram for the normalized values of kinetic energy of currents near Crimea (point 3).

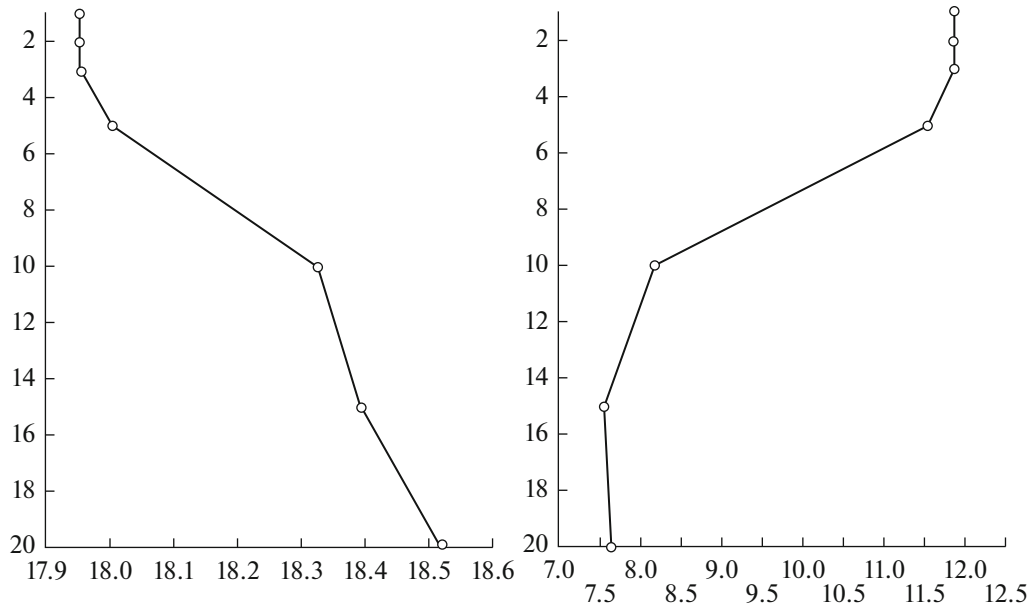


Fig. 8. Mean profiles of salinity (left panel: the horizontal axis shows salinity in per mille) and temperature (right panel: the horizontal axis shows temperature in degrees Celsius) at the stations near the Antalia coast (based on the results of the numerical modeling for April). The vertical axis is depth in meters.

the pattern of subinertial oscillations is complicated by the trapped and inertial-gravity waves appearing near the shelf.

The coherence between the fluctuations of sea surface height at different stations is high at a period of 6 h. The distribution of coherences between currents becomes more consistent as the depth increases. This provides evidence about the existence of baroclinic seiche oscillations caused by the baroclinic tides [1]. These oscillations cover the entire eastern “corner” of the sea.

Low coherence is frequently observed between the fluctuations of currents at periods of 6, 8, and 12 h at

the stations of the shelf and open sea. It is shown in [1] on the basis of the field data that the spectral density in the internal layers increases from low frequencies to the local inertial frequency and then the energy decreases with individual peaks in the high-frequency range (1–12 h). Thus, long-period waves cover the entire water column of the sea and propagate over long distances. At the stations near the coast, the energy of low-frequency oscillations in the sea surface height field sometimes exceeds the energy of the inertial motion by one order of magnitude, which is caused by the influence of the edge waves in the surface layer of the sea.

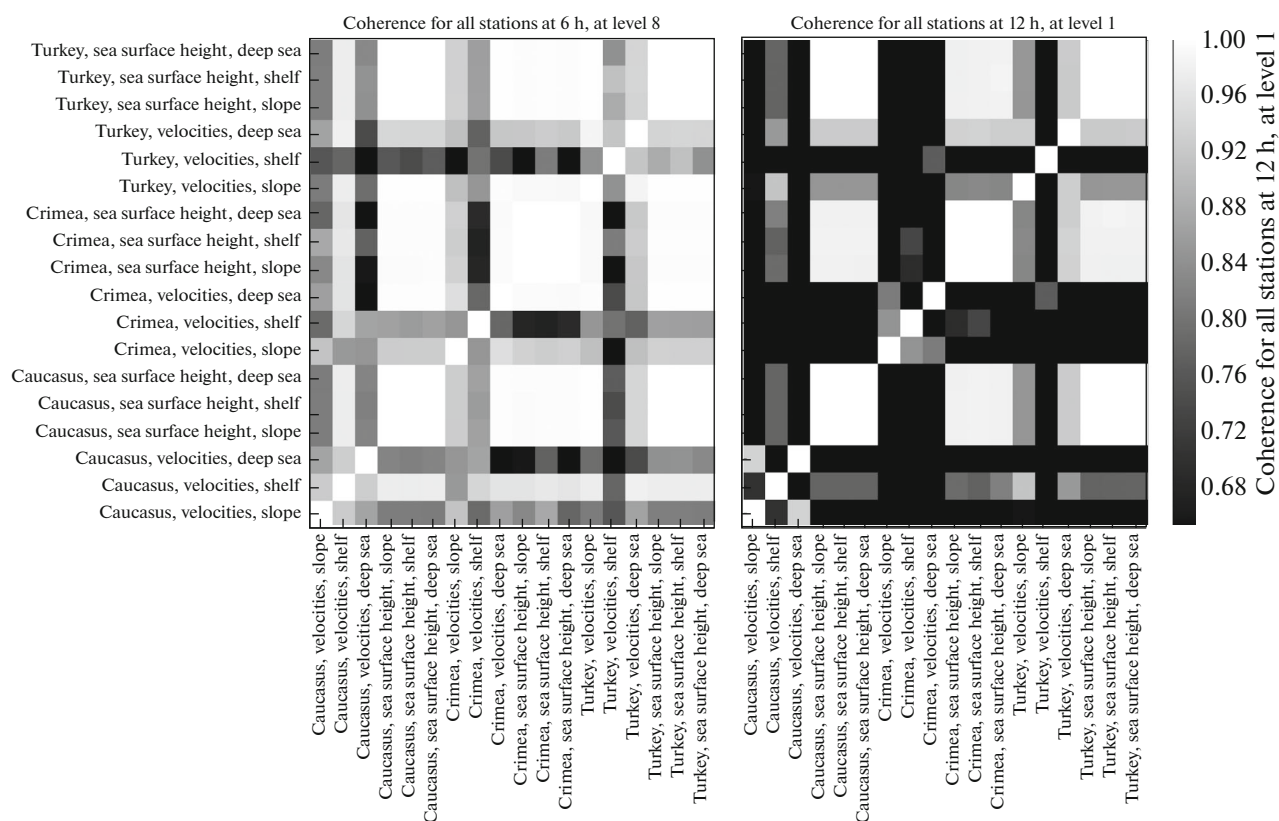


Fig. 9. Example of coherence matrices at a period of 6 h (the eighth level, left panel) and 12 h (the first level, right panel).

4. CONCLUSIONS

- Accounting for the semidiurnal tidal potential in the model not only improves the accuracy of simulations of sea surface height at the coastal stations but also generates subinertial baroclinic oscillations, which were previously revealed in the Black Sea from a series of in situ observations.

- The power of the tidal potential not only increases the energy of fluctuation processes in the sea but also generates additional oscillations of the currents in the shelf and continental slope regions.

- The development of semidiurnal tidal oscillations generates baroclinic oscillations of currents in the entire water column of the sea at a frequency of 12-h tide (the so-called baroclinic tide), which in turn generate local seiche oscillations determined by the coast configuration and bottom topography.

- Values of the natural inertial oscillations may be different from the theoretical value due to the vorticity of background currents and influence of the edge waves.

- The model reveals the existence of inertial-gravity waves of the subinertial period with the wave vector directed at a specific angle to the vertical in the direction from the bottom to the surface.

ACKNOWLEDGMENTS

This research was supported by the State Task, theme no. 0827-2014-0010.

REFERENCES

- A. S. Blatov and V. A. Ivanov, *Hydrology and Hydrodynamics of the Shelf Zone of the Black Sea (the case the Southern Coast of Crimea)* (Naukova Dumka, Kiev, 1992) [in Russian].
- V. A. Ivanov, "Spatial and temporal variability and monitoring of hydrophysical fields of the Black Sea," *Izv., Atmos. Ocean. Phys.* **50** (1), 26–34 (2014).
- G. I. Marchuk and B. E. Paton, "The Black Sea as a simulation ocean model," *Russ. J. Numer. Anal. Math. Modell.* **27** (1), 1–4 (2012).
- V. B. Zalesny, A. V. Gusev, and S. N. Moshonkin, "Numerical model of the hydrodynamics of the Black Sea and the Sea of Azov with variational initialization of temperature and salinity," *Izv., Atmos. Ocean. Phys.* **49** (6), 642–658 (2013).
- V. B. Zalesny, A. V. Gusev, and V. I. Agoshkov, "Modeling Black Sea circulation with high resolution in the coastal zone," *Izv., Atmos. Ocean. Phys.* **52** (3), 277–293 (2016).
- G. I. Marchuk, *Methods of Numerical Mathematics* (Springer, New York, 1982; Lan^o, St. Petersburg, 2009).

7. J. M. Stanev and J. M. Beckers, "Barotropic and baroclinic oscillations in strongly stratified basins. Numerical study of the Black Sea," *J. Mar. Syst.* **19**, 65–112 (1999).
8. M. Assovskiy and V. Agoshkov, "Numerical simulation of general World Ocean dynamics subject to tide-forming forces," *Russ. J. Numer. Anal. Math. Modell.* **26** (2), 113–141 (2011).
9. N. A. Diansky, V. V. Fomin, N. V. Zhokhova, and A. N. Korshenko, "Simulations of currents and pollution transport in the coastal waters of Big Sochi," *Izv., Atmos. Ocean. Phys.* **49** (6), 611–621 (2013).
10. A. A. Kordzadze and D. I. Demetrashvili, "Kratkosrochnyi prognoz gidrofizicheskikh polei v vostochnoi chasti Chernogo morya," *Izv., Atmos. Ocean. Phys.* **49** (6), 674–685 (2013).
11. G. K. Korotaev, V. V. Knysh, and A. I. Kubryakov "Study of formation process of cold intermediate layer based on reanalysis of Black Sea hydrophysical fields for 1971–1993," *Izv., Atmos. Ocean. Phys.* **50** (1), 35–48 (2014).
12. V. B. Zalesny, N. A. Diansky, V. V. Fomin, S. N. Moshonkin, and S. G. Demyshev, "Numerical model of the circulation of the Black Sea and the Sea of Azov," *Russ. J. Numer. Anal. Math. Modell.* **27** (1), 95–111 (2012).
13. G. I. Marchuk, B. E. Paton, G. K. Korotaev, and V. B. Zalesny, "Data-computing technologies: A new stage in the development of operational oceanography," *Izv., Atmos. Ocean. Phys.* **49** (6), 579–591 (2013).
14. V. I. Agoshkov, E. I. Parmuzin, and V. P. Shutyaev, "Assimilyatsiya dannykh nablyudenii v zadache tsirkulyatsii Chernogo morya i analiz chuvstvitel'nosti ee resheniya," *Izv., Atmos. Ocean. Phys.* **49** (6), 592–602 (2013)
15. <http://data1.gfdl.noaa.gov>. Accessed January 26, 2016.
16. A. N. Lukyanova, A. V. Bagaev, T. V. Plastun, N. V. Markova, V. B. Zalesny, and V. A. Ivanov, "The Black Sea deepwater circulation research by results of numerical modeling and in-situ data: INM RAS model numerical experiment," *Ekol. Bezop. Pribrezhn. Shel'f. Zon Morya*, No. 3, 9–14 (2016).
17. A. Defant, *Physical Oceanography*, Vol. 2 (Pergamon, New York, 1961).
18. A. V. Zalesny, A. N. Gusev, V. V. Lukyanova, and V. V. Fomin, "Numerical modelling of sea currents and tidal waves," *Russ. J. Numer. Anal. Math. Modell.* **31** (2), 115–125 (2016).
19. S. Chen, J. Hu, and J. A. Polton, "Features of near-linear motions observed on the northern South China shelf during the passage of two typhoons," *Acta Oceanol. Sin.* **34** (1), 38–43 (2015).
20. B. Yang, Y. Hou, and P. Hu, "Observed near-inertial waves in the wake of Typhoon Hagupit in the northern South China Sea," *Chin. J. Oceanol. Limnol.* **33** (5), 1265–1278 (2015).
21. S. G. Demyshev, O. A. Dymova, N. V. Markova, and V. B. Piotukh, "Numerical experiments on modeling the Black Sea deep currents," *Morsk. Gidrofiz. Zh.*, No. 2, 38–52 (2016).

Translated by E. Morozov

Reproduced with permission of copyright owner. Further reproduction prohibited without permission.